Eur. Phys. J. E **19**, 471–476 (2006)
DOI 10.1140/epje/i2005-10076-8

THE EUROPEAN PHYSICAL JOURNAL E

Preparation and characterization of (PVP + $NaClO_4$) electrolytes for battery applications

Ch.V. Subba Reddy, A.-P. Jin, Q.-Y. Zhu, L.-Q. Mai, and W. Chen[a]

Institute of Materials Science and Engineering, Wuhan University of Technology, Wuhan, 430-070, PRC

Received 28 June 2005 and Received in final form 19 December 2005 /
Published online: 10 April 2006 –

Abstract. A sodium ion-conducting polymer electrolyte based on polyvinyl pyrrolidone (PVP) complexed with $NaClO_4$ was prepared using the solution-cast technique. The cathode film of V_2O_5 xerogel modified with polyvinyl pyrrolidone was prepared using the sol-gel method. Investigations were conducted using X-ray diffractometry (XRD), Fourier transformation infrared (FT-IR) spectroscopy. The ionic conductivity and transference number measurements were performed to characterize the polymer electrolyte for battery applications. The transference number data indicated that the conducting species in these electrolytes are the anions. Using the electrolyte, electrochemical cells with a configuration $Na/(PVP + NaClO_4)/V_2O_5$ modified by (PVP) were fabricated and their discharge profiles studied.

PACS. 82.35.Rs Polyelectrolytes – 66.30.Dn Theory of diffusion and ionic conduction in solids – 82.45.Gj Electrolytes – 82.47.Aa Lithium-ion batteries

1 Introduction

Polymer electrolytes are currently of interest owing to their advantageous and special mechanical properties, *i.e.*, ease of fabrication as thin films of desirable sizes and suitability for electrode-electrolyte contacts in different electrochemical devices. Interest began in this field after the studies of materials based on alkali metal salts complexed with polyethylene oxide (PEO) reported by Wright and co-workers [1,2] and Armand *et al.* [3,4]. Polymer blend electrolytes consisting of (PVP + PVA) and alkali metal salts have been used to make electrochemical cells [5–7]. A relatively small number of studies have been reported on the development of PVP electrolytes for solid-state batteries.

A few attempts have tried electrolytes based on sodium complexed films. Apart from the scientific interest, the use of sodium has several advantages over their lithium counterparts. Sodium is available in abundance at a cheaper cost than lithium. It may be possible to obtain solid electrolytes of sufficiently high conductivity because sodium does not form an alloy with aluminium, making it possible to use this metal as current collector instead of the costlier and heavier nickel. Furthermore, the softness of these materials makes it easier to achieve and maintain contact with other components in the battery. Investigations have also been made on sodium ion-conducting polymer electrolytes based on PEO, polypropylene oxide (PPO), and polybismethoxy ethoxy phosphazene (MEEP) complexed with NaI, $NaClO_4$, NaSCN, and $NACF_3SO_3$ [8–10]. Several researchers have reported on plasticized polymer electrolytes with enhanced ionic conductivity in PVC-based polymer electrolytes [11–17].

Recent research trends in the field of rechargeable lithium batteries are directed towards the development of cells with high-energy density (Wh/kg) and high-power density [18]. To achieve a high amount of energy stored in a given mass or volume, it is usually desirable that the number of available charge carriers per mass or volume unit is as high as possible. The capacity for energy storage in a rechargeable lithium cell is mainly dependent on the cathode materials. The most studied cathode materials for lithium batteries are crystalline cobalt-, manganese- and nickel-based oxides [19]. As part of continuing efforts to improve the capacity of cathode materials, attempts to synthesize transition-metal oxides with an amorphous nature and high surface area, such as the xerogel and aerogel forms, have been made from V_2O_5 [20–24] and MnO_2 [25]. Hybridization of the layered inorganic cathode materials with electrochemically active organic polymers is regarded as another interesting approach to improve the capacity for electrochemical lithium insertion. Intercalating organic molecules into the layered inorganic host materials can produce inorganic-organic hybrid materials. Many studies have modified V_2O_5 with polyaniline (PANI), poly (ethylene glycol) (PEG), polypyrrole (PPY) and poly (ethylene oxide) (PEO) [26–32]. A comparatively limited research

[a] e-mail: chenw@mail.wut.edu.cn; Tel.: +86-27-878651107; Fax: +86-27-87864580.

has been done on modifying V_2O_5 xerogel with poly (vinyl pyrrolidone) (PVP). In the present paper, solid-state electrochemical cells based on (PVP + $NaClO_4$) electrolyte films are fabricated. Several experimental techniques such as temperature-dependent conductivity in the temperature range 298–423 K and transference number measurements are employed to characterize these polymer electrolyte films.

2 Experimental

Films (thickness $\approx$ 100 μm) of pure PVP and various compositions of complexed films of PVP with a salt of $NaClO_4$ were prepared with the following weight percent ratios (90 : 10), (80 : 20) and (70 : 30) using the solution-cast technique. Pure and doped polymers were dissolved in dimethyl formamide (DMF) and stirred at room temperature for 10–12 h. The stirred solutions were cast into polypropylene dishes and allowed to evaporate slowly at 353 K followed by vacuum drying.

Melting V_2O_5 powder at 875 K in a ceramic crucible results in a molten liquid [33–35]. When the molten liquid was quickly poured into distilled water, a brownish V_2O_5 solution was formed. The solution viscosity is directly related to the amount of V_2O_5 powder with respect to the water volume. The PVP solution was mixed with the V_2O_5 solution to form a mixed sol. The molar ratio of PVP to V_2O_5 was $x : 1$ ($x = 0, 0.5$). Indium tin oxide (ITO) conducting glass substrates were dipped into the mixed sol and then pulled out slowly. The xerogel formed on the glass substrate was left to dry for 48 h at room temperature. The final films were subjected to heat treatment (373 K) for 24 h in an N_2 atmosphere to maintain at a constant weight, by removing free water in the films [34].

The XRD patterns of the films were made with a HZG4/B-PC X-ray diffractrometer with CoKα radiation and graphite monochrometer. Fourier transformation infrared (FT-IR) spectra of the films were recorded using a 60-SXB IR spectrometer with a resolution of 4 cm^{-1}. The measurements were taken over a wave number range of 400–4000 cm^{-1}.

The ac impedance measurements of the polymer electrolytes were performed using an Agilent 4294A precision impedance analyzer in the range from 40 Hz to 100 kHz and temperature range 298–423 K. The measurement cell was prepared by sandwiching the polymer electrolyte film between two stainless-steel electrodes and assembled into a homemade sample holder. The transport number was evaluated using the technique described by Linford [36]. In this technique a freshly prepared film of (PVP + $NaClO_4$) was polarized in a configuration of C/(PVP + $NaClO_4$)/C under a dc bias potential of 1.5 V. The resulting current was monitored as a function of time using a Keithley electrometer. The cationic transference number is given by

$$\tau_+ = I_{+\infty}/I_{\mathrm{T}}.$$

Here $I_{+\infty}$ is the cationic current at saturation and I_{T} is the total ionic current at time zero.

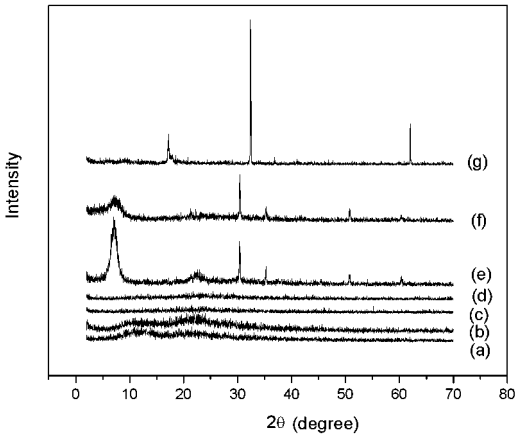

Fig. 1. XRD patterns of $NaClO_4$ complexed PVP: (a) pure PVP; (b) (PVP + $NaClO_4$) (90 : 10); (c) (PVP + $NaClO_4$) (80 : 20); (d) (PVP + $NaClO_4$) (70 : 30); (e) V_2O_5 before modification; (f) V_2O_5 after modification and (g) pure $NaClO_4$.

Solid-state electrochemical cells were fabricated with a configuration of Na/(PVP + $NaClO_4$)/(PVP + V_2O_5). Details of the fabrication of the electrochemical cell are given elsewhere [37]. The discharge characteristics of the cells were monitored under a constant load of 100 kΩ.

3 Results and discussion

3.1 XRD analyses

The XRD patterns of pure PVP, $NaClO_4$, complexed PVP, and V_2O_5 xerogels both before and after modification with PVP are presented in Figure 1. The diffraction peaks are less intense in $NaClO_4$ complexed PVP compared to the pure PVP. This shows a decrease in the degree of crystallinity of the polymer after the addition of $NaClO_4$. Peaks corresponding to uncomplexed PVP are also present together with that of $NaClO_4$ in complexed PVP showing the simultaneous presence of both uncomplexed and complexed PVP phases. No sharp peaks were observed for higher concentrations of the $NaClO_4$ salt in the polymer, suggesting the dominant presence of an amorphous phase. No peak corresponding to $NaClO_4$ is observed in the higher compositions of the complexed PVP, which indicates the absence of excess salt (uncomplexed) in the material. In summary, these observations confirm the complexation of the $NaClO_4$ salt with the polymer PVP. The XRD pattern of the unmodified V_2O_5 xerogel shows four peaks whose d values are 12.3803, 3.9376, 2.9402 and 1.7979 Å corresponding to diffraction by the (001), (003), (004) and (006) crystal planes, respectively [38]. No ($hk0$) and (hkl) reflections are observed in Figure 1, confirming the turbostratic nature of the V_2O_5 slabs perpendicular to the stacking axis. The repeated distance in the modified V_2O_5 xerogel film increases from 12.3803 Å to 13.283 Å. The increase of the repeat distance is thought to result from PVP being intercalated into the V_2O_5 xerogel interlayer and increasing the spacing between the V_2O_5 xerogel layers [39,40].

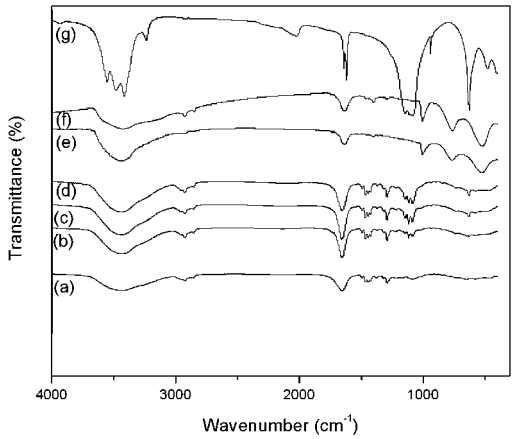

Fig. 2. IR spectra of $NaClO_4$ complexed PVP: (a) pure PVP; (b) (PVP + $NaClO_4$) (90 : 10); (c) (PVP + $NaClO_4$) (80 : 20); (d) (PVP + $NaClO_4$) (70 : 30); (e) V_2O_5 before modification; (f) V_2O_5 after modification and (g) pure $NaClO_4$.

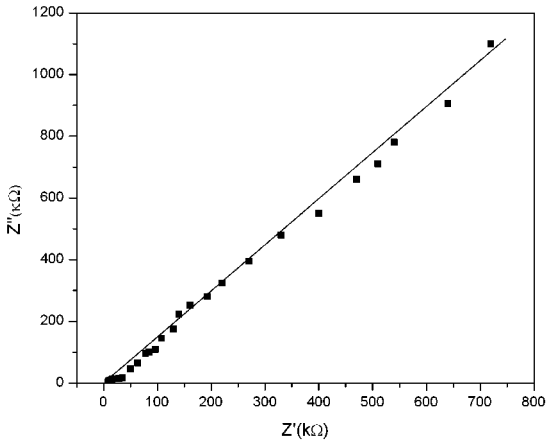

Fig. 3. Impedance plot of the (PVP + $NaClO_4$) (90 : 10) polymer electrolyte at ambient temperature.

3.2 IR analyses

The IR spectra of pure PVP, $NaClO_4$ complexed PVP of different compositions, $NaClO_4$, V_2O_5 xerogel, both before and after modification with PVP, are shown in Figure 2. The following changes in the spectral feature have been observed after comparing the spectrum of complexed PVP with that of the pure PVP and $NaClO_4$. The intensity of the aliphatic C-H stretching vibrational band observed around 2900 cm^{-1} in PVP is found to decrease with increasing concentration of the $NaClO_4$ salt in the polymer matrix. The width of the C=O stretching band observed around 1100 cm^{-1} in PVP also showed a decrease with an increase of $NaClO_4$ in the polymer. Furthermore, new peaks around 3941, 1373, 1147, 941 and 637 cm^{-1} have been observed in complexed PVP. The peaks at 1172 and 652 cm^{-1} corresponding to PVP, and the peaks at 3552, 3481, 3237, 2025, 1617 and 479 cm^{-1} corresponding to $NaClO_4$ disappeared in complexed PVP. The appearance of new peaks along with changes in existing peaks (and/or their disappearance) in IR spectra is a direct indication of the complexation of PVP with $NaClO_4$

There is a broad band at 3441 cm^{-1} corresponding to the O-H vibration from water [26], which confirms the presence of water in the V_2O_5 xerogel before modification with PVP. The V_2O_5 xerogel also exhibits three main vibration modes in the 400–1007 cm^{-1} region. The terminal oxygen symmetric stretching mode (ν_s) of V=O and the bridge oxygen asymmetric and symmetric stretching modes (ν_{as} and ν_s) of V-O-V are at 1007, 764 and 527 cm^{-1}, respectively [27]. IR spectra after modification with PVP show characteristic intense peaks at 1166, 1293, 1375 and 1400 cm^{-1} which proves that PVP is present and the poorly resolved peak at 3652 cm^{-1} is an indication that amorphous PVP is present.

All the peaks change to varying extents when intercalating PVP into the V_2O_5 xerogel. The ν_s (V-O-V) and ν_{as} (V-O-V) modes shift to lower wave numbers. The ν_{as} (V-O-V) mode shifts from 764 cm^{-1} to 754 cm^{-1} and its intensity increases. The ν_s (V-O-V) mode moves from 527 cm^{-1} to 522 cm^{-1}. In contrast, the ν_s (V=O) band shifts to a slightly higher wave number, from 1007 cm^{-1} to 1012 cm^{-1}. There are two types of vibration modes. These shifts indicate the nature of the modification. The shift of the ν_s (V=O) mode indicates that H-bonding effects are observed in the modified hybrid V_2O_5 xerogel [18]. Namely, the H atoms in PVP are H-bonded with the O atoms of the V=O bonds of V_2O_5 xerogel. The second type of vibration mode affected by the modification is the V-O-V stretch. For the existence of H-bonds, the position of the V atom in the xerogel changes due to the V=O bond being weakened [41], which causes a strengthening of the V-O-V bond. All these observations suggest that PVP is intercalated in the interlayer spacing of the V_2O_5 xerogel and has a relatively strong interaction with the V_2O_5 xerogel, which is in good agreement with the XRD results.

3.3 Conductivity studies

The ionic conductivity has been determined from the ac impedance analysis using the cell with blocking electrodes as described in the experimental section. The typical impedance plot of (PVP + $NaClO_4$)(90 : 10) at ambient temperature is shown in Figure 3. The bulk resistance was measured from the high-frequency intercept on the real axis. The conductivity of the polymer electrolyte was calculated from the measured resistance, area and thickness of the polymer film.

Figure 4 shows the Arrhenius plots of logarithmic conductivity *versus* inverse temperature for pure PVP and for different compositions of (PVP + $NaClO_4$) polymer electrolyte over the temperature range 298–423 K. The following features are observed:

1) The ionic conductivity increases with temperature in pure PVP and also for all the compositions of the (PVP + $NaClO_4$) polymer electrolyte system.
2) The conductivity values do not show any abrupt jump with temperature which indicates that these electrolytes exhibit a completely amorphous structure [42],

Table 1. Various cell parameters for ($PVC + NaClO_4$) polymer electrolyte cells.

Cell parameters	$Na/(PVP + NaClO_4)$ $(90:10)/(PVP + V_2O_5)$	$Na/(PVP + NaClO_4)$ $(90:10)/(V_2O_5)$
Effective area of the electrolyte (cm^2)	2.00	2.00
Cell weight (gm)	0.50	0.50
Open-circuit voltage (OCV) (V)	1.89	2.11
Short-circuit current (SCC) (μA)	105	120
Load (kΩ)	100	100
Current density ($\mu A/cm^2$)	52.50	60.00
Discharge time for plateau region (h)	40	48
Power density (mW/kg)	41.16	64.48
Energy density (mWh/kg)	1646.40	3095.28

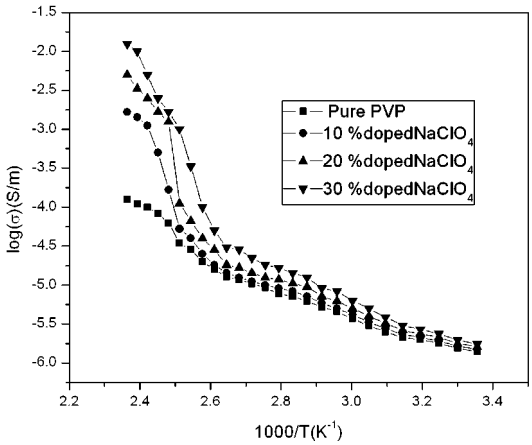

Fig. 4. Log plots of conductivity *versus* $1000/T$ for ($PVP + NaClO_4$) polymer electrolytes.

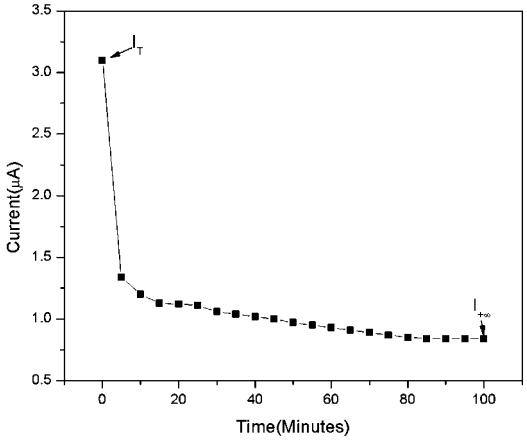

Fig. 5. Current *versus* time plot of ($PVP + NaClO_4$) (80 : 20) polymer electrolyte system.

which is confirmed from XRD studies. The increase in conductivity with temperature can be linked to the decrease in viscosity and thus, to the increased chain flexibility [43]. Since the conductivity-temperature data obeys an Arrhenius relationship, the nature of cation transport is quite similar to that occurring in ionic crystals, where ions jump into neighbouring vacant sites and hence increase the ionic conductivity [44]. The activation energy (E_a), which is a combination of the energy of defect formation and of the energy of defect migration can be calculated from the plots. The activation energy for the PVP, ($PVP + NaClO_4$)(90 : 10); (80 : 20); (70 : 30) samples is 0.72, 0.54, 0.38 and 0.26 eV, respectively. The low activation energy for the sodium ion transport is due to the completely amorphous nature of the polymer electrolytes that facilitate the fast Na^+ ion motion in the polymer network. The completely amorphous nature also provides a bigger free volume in the polymer electrolyte system with increasing temperature [42].

3.4 Transference number

The transference number of the sodium ion in the polymer electrolytes is around 0.27. This implies that the major conducting species in these electrolytes is the anion ClO_4^-. The polarization current saturates at ~ 0.84 (Fig. 5). The saturated polarization current is the cationic current according to reference [36]; the anionic current has been impeded by concentration polarization.

3.5 Discharge characteristics

The first discharge curves for the V_2O_5 xerogels both before and after modification with PVP are given in Figure 6. The discharge capacity of the modified xerogel film is lower than that of the unmodified V_2O_5 xerogel, *i.e.* 1856 μAh/g for the modified V_2O_5 xerogel compared to 1248 μAh/g. This tendency for a decrease in the discharge capacity has been observed previously for as-prepared organic/V_2O_5

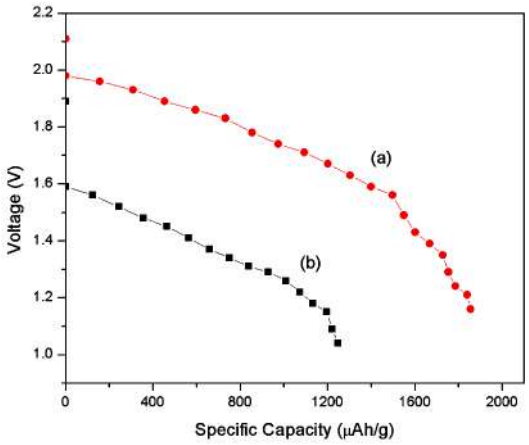

Fig. 6. Initial discharge curves of as-prepared (a) V_2O_5; (b) PVP/V_2O_5.

hybrid materials [26,27,29,30]. This might be due to a decreased average vanadium oxidation state as a result of the intercalation of organic polymers and/or poor electroactivity of intercalated polymers toward lithium insertion.

The open-circuit voltages (OCVs) and short-circuit currents (SCCs) were respectively found to be 1.89 V and 105 μA for the modified V_2O_5 xerogel cell, and 2.11 V and 120 μA for the unmodified V_2O_5 xerogel cell. Several other profiles of the cells were evaluated and are given in Table 1.

From Table 1, it is clear that the SCC and the discharge time for the plateau region are found to be greater in the unmodified V_2O_5 xerogel cell compared with the modified V_2O_5 xerogel cell, indicating that unmodified V_2O_5 xerogel cells are more stable than the modified V_2O_5 xerogel cells. Further work is in progress to improve the discharge capacity of the modified V_2O_5 xerogel cell by post-treatment with oxygen.

4 Conclusions

PVP has been intercalated into V_2O_5 xerogels. The intercalation is confirmed by X-ray diffraction and FT-IR spectroscopy. The modified V_2O_5 xerogel cell exhibits a lower discharge capacity than the unmodified V_2O_5 xerogel cell. Conductivity-temperature studies indicate that the ionic transport is similar to that in ionic crystals, *i.e.* hopping from one defect site to another. The value of the activation energy decreases with increasing ionic conductivity and vice versa. The transference number data has indicated that the conduction in these electrolytes is due to anions. Unmodified V_2O_5 xerogel cells were found to be more stable than modified V_2O_5 xerogel cells.

One of the authors (Ch.V. Subba Reddy) wishes to thank the Wuhan University of Technology Management for the financial support in the form of a Post-Doctoral Fellowship to carry out the above work. The Opening Foundation of Hubei Ferroelectric and Piezoelectric Materials and Devices Key Laboratory supported this work.

References

1. P.V. Wright, Br. Polym. J. **7**, 319 (1975).
2. D.E. Fenton, J.M. Parker, P.V. Wright, Polymer **14**, 589 (1973).
3. M.B. Armand, J.M. Chabagno, M. Duclot, in *Fast Ion Transport in Solids*, edited by P. Vashishta, J.N. Mundy, G.K. Shenoy (North Holland, Amsterdam, 1979) p. 131.
4. M.B. Armand, J.M. Chabagno, M. Duclot, *International Conference on Solid Electrolytes, Ext. Abstract, University of St. Andrews, Scotland, 1988.*
5. Ch.V. Subba Reddy, A.K. Sharma, V.V.R. Narasimha Rao, J. Mater. Sci. Lett. **21**, 105 (2002).
6. Ch.V. Subba Reddy, A.K. Sharma, V.V.R. Narasimha Rao, J. Power Sources **111**, 357 (2002).
7. Ch.V. Subba Reddy, A.K. Sharma, V.V.R. Narasimha Rao, J. Ionics **10**, 142 (2004).
8. D. Fautex, M.D. Lupien, C.D. Robitaille, J. Electrochem. Soc. **134**, 2761 (1987).
9. S.G. Greenbaum, Y.S. Pak, M.C. Wintersgill, J.J. Fontanella, J.W. Schultz, J. Electrochem. Soc. **135**, 235 (1988).
10. S.G. Greenbaum, K.J. Ademic, Y.S. Pak, M.C. Wintersgill, J.J. Fontanella, Solid State Ionics **28-30**, 1042 (1988).
11. M. Alamgir, K.M. Abraham, J. Electrochem. Soc. **140**, L96 (1993).
12. A.M. Sukeshini, A. Nishimoto, M. Watanabe, Solid State Ionics **86-88**, 385 (1996).
13. H.J. Rhoo, H.T. Kim, J.K. Park, T.S. Hwang, Electrochim. Acta **42**, 1571 (1997).
14. A. Manuel Stephan, R. Thirunakaran, N.G. Renganathan, V. Sundram, S. Pitchumani, N. Muniyandi, R. Gangadharan, P. Ramamoorthy, J. Power Sources **82**, 752 (1999).
15. S. Ramesh, A.K. Arof, Solid State Ionics **136-137**, 1197 (2000).
16. A. Manuel Stephan, T. Prem Kumar, N.G. Renganathan, S. Pitchumani, R. Thirunakaran, N. Muniyandi, J. Power Sources **89**, 80 (2000).
17. S. Ramesh, A.H. Yahaya, A.K. Arof, Solid State Ionics **152-153**, 291 (2002).
18. B.B. Owens, W.H. Smyrl, J.J. Xu, J. Power Sources **81-82**, 150 (1999).
19. M. Winter, J.O. Besenhard, M.E. Spahr, P. Novak, Adv. Mater. **10**, 725 (1998).
20. D.B. Le, S. Passerini, A.L. Tipton, B.B. Owens, W.H. Smyrl, J. Electrochem. Soc. **142**, L102 (1995).
21. D.B. Le, S. Passerini, J. Guo, J. Ressler, B.B. Owens, W.H. Smyrl, J. Electrochem. Soc. **143**, 2099 (1996).
22. F. Coustier, S. Passerini, W.H. Smyrl, J. Electrochem. Soc. **145**, L73 (1998).
23. S. Passerini, J.J. Ressler, D.B. Le, B.B. Owens, W.H. Smyrl, Electrochim. Acta **44**, 2209 (1999).
24. B.B. Owens, S. Passerini, W.H. Smyrl, Electrochim. Acta **45**, 215 (1999).
25. J.J. Xu, A.J. Kinser, B.B. Owens, W.H. Smyrl, Electrochem. Solid State Lett. **1**, 1 (1998).
26. F. Leroux, B.E. Koene, L.F. Nazar, J. Electrochem. Soc. **143**, L181 (1996).
27. F. Leroux, G. Goward, W.P. Power, L.F. Nazar, J. Electrochem. Soc. **144**, 3886 (1997).
28. J. Harreld, H.P. Wong, B.C. Dave, B. Dunn, L.F. Nazar, J. Non-Cryst. Solids **225**, 319 (1998).

29. H.P. Wong, B.C. Dave, F. Leroux, J. Harreld, B. Dunn, L.F. Nazar, J. Mater. Chem. **8**, 1019 (1998).
30. G. Goward, F. Leroux, L.F. Nazar, Electrochim. Acta **43**, 1307 (1998).
31. M. Lira-Cantu, P. Gomez-Romero, J. Electrochem. Soc. **146**, 2029 (1999).
32. J.H. Harreld, B. Dunn, L.F. Nazar, Int. J. Inorg. Mater. **1**, 135 (1999).
33. G.Y.D. Chuan, X. Niakan, Z. Xiulin, Mater. Res. Bull. **31**, 335 (1996).
34. Z.S.E. Mandouh, M.S. Selim, Thin Solid Films **259**, 371 (2000).
35. F. Leroux, B.E. Koene, L.F. Nazar, J. Electrochem. Soc. **144**, 3886 (1997).
36. R.G. Linford, in *Solid State Ionic Devices*, edited by B.V.R. Chowdari, S. Radhakrishna (World Scientific, Singapore, 1986) p. 551.
37. P. Prosini, S. Passerini, R. Vellone, W.H. Smyrl, J. Power Sources **75**, 73 (1998).
38. N. Ozer, Thin Solid Films **80**, 305 (1997).
39. W. Chen, Q. Xu, R.Z. Yuan, Mater. Sci. Eng. B **15**, 77 (2000).
40. F.J. Anaissi, G.J.F. Demets, H.E. Toma, Electrochem. Commun. **1**, 332 (1999).
41. T.Yao, Y.Oka, N. Yamamoto, Mater. Res. Bull. **27**, 669 (1992).
42. M.S. Michael, M.M.E. Jacob, S.R.S. Prabaharan, S. Radhakrishna, Solid State Ionics **98**, 167 (1997).
43. S.S. Sekhon, K.V. Pradeep, S.A. Agnihotry, in *Solid State Ionics: Science and Technology*, edited by B.V.R. Chowdari, K. Lal, S.A. Agnihotry, N. Khare, S.S. Sekhon, P.C. Srivastava, S. Chandra (World Scientific, Singapore, 1998) pp. 217-221.
44. J.L. Souquet, M. Levy, M. Duclot, Solid State Ionics **70-71**, 337 (1994).